OpenAccess

ORIGINAL ARTICLE

GOCE gradiometer: estimation of biases and scale factors of all six individual accelerometers by precise orbit determination

P. N. A. M. Visser

Abstract A method has been implemented and tested for estimating bias and scale factor parameters for all six individual accelerometers that will fly on-board of GOCE and together form the so-called gradiometer. The method is based on inclusion of the individual accelerometer observations in precise orbit determinations, opposed to the baseline method where so-called common-mode accelerometer observations are used. The method was tested using simulated data from a detailed GOCE system simulator. It was found that the observations taken by individual accelerometers need to be corrected for (1) local satellite gravity gradient (SGG), and (2) rotational terms caused by centrifugal and angular accelerations, due to the fact that they are not located in the satellite's center of mass. For these corrections, use is made of a reference gravity field model. In addition, the rotational terms are derived from on-board star tracker observations. With a perfect a priori gravity field model and with the estimation of not only accelerometer biases but also accelerometer drifts, scale factors can be determined with an accuracy and stability better than 0.01 for two of the three axes of each accelerometer, the exception being the axis pointing along the long axis of the satellite (more or less coinciding with the flight direction) for which the scale factor estimates are unreliable. This axis coincides with the axis of drag-free control, which results in a small variance of the signal to be calibrated and thus an inaccurate determination of its scale factor in the presence of relatively large (colored) accelerometer observation errors. In the presence of gravity field model errors, it was found that still an accuracy and stability of about 0.015 can be obtained

for the accelerometer scale factors by simultaneously estimating empirical accelerations.

Keywords Accelerometer · Accelerometer drift · Bias · Calibration · GOCE · Gradiometer · Precise orbit determination · Scale factor

1 Introduction

The gravity field and steady-state ocean circulation explorer (GOCE) will be the first European Space Agency (ESA) core earth explorer mission. The foreseen launch date of GOCE is in the second half of 2008 (as of May 2008). GOCE aims at modeling the static earth's gravity field with an accuracy of 2 cm in geoid and 1 mGal in gravity anomaly at a spatial resolution or half-wavelength of 100 km (Drinkwater et al. 2007). GOCE will carry as primary science instrument a gradiometer, consisting of three pairs of accelerometers on orthogonal axes (Fig. 1). The X axis is aligned with the long axis of the satellite, the Z axis is perpendicular to the X axis and is aligned with the wings of the GOCE satellite, and the Y axis completes an orthonormal frame. The orientation of these axes is derived from star tracker observations (Sect. 2). The location and orientation of the star trackers with respect to the gradiometer axes is determined accurately before launch. The GOCE satellite will be predominantly earth-pointing with yaw angles up to 3° (cf. Fig. 3 in Visser 2007a). The gradiometer will observe local satellite gravity gradients with high precision in a measurement bandwidth (MB) of 0.005–0.1 Hz. In addition, GOCE will be equipped with a dual-frequency Lagrange GPS receiver (Banfi et al. 2000) for precise orbit determination and for providing information of the longer wavelengths of the earth's gravity field. A drag-free control (DFC) system will reduce

P. N. A. M. Visser (✉)
Delft Institute of Earth Observation and Space Systems (DEOS),
Delft University of Technology, Kluyverweg 1, 2629 HS,
Delft, The Netherlands
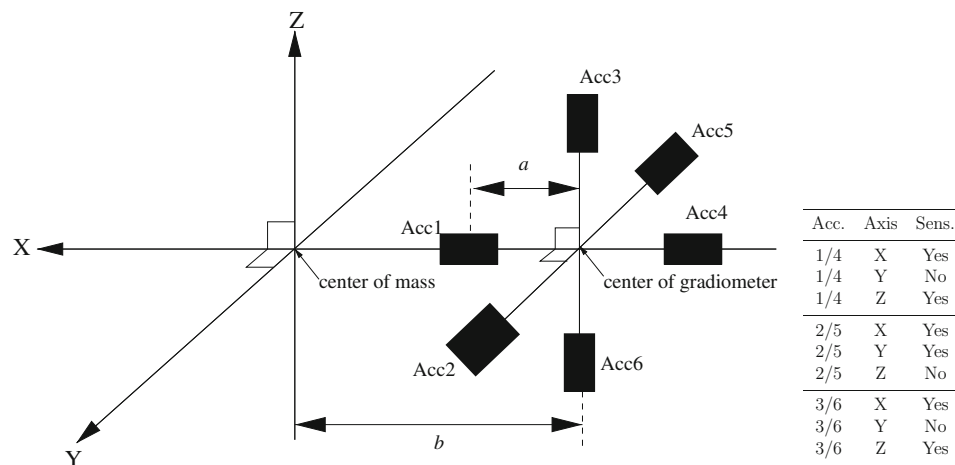e-mail: P.N.A.M.Visser@tudelft.nl

Acc.	Axis	Sens.
1/4	X	Yes
1/4	Y	No
1/4	Z	Yes
2/5	X	Yes
2/5	Y	Yes
2/5	Z	No
3/6	X	Yes
3/6	Y	No
3/6	Z	Yes

Fig. 1 Configuration and naming convention of the three orthogonal pairs of accelerometers that form together a gravity gradiometer. Half the arm length of each pair is equal to *a* (nominally 50 or 51.4 cm, Cesare and Catastini 2005), whereas the offset of the center of the gradiometer with respect to the center of mass of the satellite is indicated by *b* (nominally of the order of a few cm, in the figure the offset is assumed to be along the *X* axis only). The locations of the accelerometers are indicated along the *X*, *Y* and *Z* axes of the gradiometer reference frame. These axes are aligned with the along-track (or flight), cross-track and radial (or height) directions, respectively, to within a few degrees. The sensitive and less sensitive axes are indicated as well

the non-gravitational accelerations in predominantly the flight direction such that the accelerometers will not get saturated (ESA 1999).

The satellite gravity gradient (SGG) observations are derived from the so-called differential mode (DM) of the individual accelerometer measurements, which need to be corrected for rotational terms (i.e. centrifugal and angular accelerations). The so-called common-mode (CM) provides a very good observation of the non-gravitational accelerations experienced by GOCE. The DM and CM observations can be represented as follows:

$$a_{DM,ij,k} = (a_{i,k} - a_{j,k})/2$$
$$a_{CM,ij,k} = (a_{i,k} + a_{j,k})/2 \tag{1}$$

where *a* represents the accelerometer observations, *i* and *j* the number of the accelerometer as indicated in Fig. 1 for the three pairs (*i*, *j* = 1, 4 or 2, 5 or 3, 6), and *k* the axis (*k* = *X*, *Y*, *Z*). Nominally, the CM observations are used in a combined orbit and gravity field determination from the GPS satellite-to-satellite tracking (SST) observations to efficiently separate gravitational from non-gravitational accelerations. Together with a gravity field model, typically CM accelerometer biases and scale factors are co-estimated (Reigber et al. 2003; Visser and van den IJssel 2003; Visser 2007a). The CM observations are the average of observations taken by pairs of accelerometers. The estimated CM biases and scale factors thus represent a combination of biases and scale factors of individual accelerometers.

In principle, the method of estimating calibration parameters for the GOCE accelerometers is based on a precise orbit determination (Montenbruck and Gill 2000) in which these calibration parameters are introduced as additional unknowns. The method is the same as typically used for deriving the observation and least-squares normal equations for CHAMP and GRACE accelerometer calibration parameters (Bruinsma and Biancale 2003; Bruinsma et al. 2004; Visser and van den IJssel 2003). Normally, the largest signal that is picked up by space-borne accelerometers on-board low-flying satellites like CHAMP and GRACE is in the along-track or flight direction, which is predominantly caused by atmospheric drag. For GOCE the situation is different because of the DFC, which aims at nullifying the non-gravitational accelerations in the flight direction thereby causing parasitic accelerations in the cross-track and radial direction. Simulations indicate that variations of the remaining non-gravitational accelerations are of the order of 50, 1,000 and 400 nm/s^2 for the *X*, *Y* and *Z* direction, respectively, displaying a noisy behavior for the *X* direction and a dominant 1 cycle-per-revolution behavior for the other two directions (cf. Fig. 2 in Visser 2007b). For GOCE, it is therefore anticipated that for example accelerometer scale factors for the radial and cross-track directions would be better observable. GOCE will also carry a new generation of accelerometers, which have a limited dynamic range (6 × 10^{-6} m/s^2), a measurement bandwidth of 0.005–0.1 Hz, but a very high sensitivity for two out of three axes (10^{-12} m/s^2) (Alenia 1999), with the 3rd axis being an order of magnitude less sensitive (i.e. a factor of 10). Below 0.005 Hz, the accelerometers are anticipated to suffer from noise that is proportional to the inverse of the frequency (so-called "one-over-f" or $1/f$ noise, with *f* the frequency). Simulations of

the behavior of the GOCE accelerometers indicate that such noise manifests itself as a slowly changing drift (see e.g. Fig. 3 of Visser 2007b). Such a drift will especially lead to relatively large orbit errors in the flight or along-track direction, which is predominantly aligned with the X axis. This can for example be proved by the Hill equations (Clohessy and Wiltshire 1960) and is also reflected by the low formal errors for estimated biases and bias drifts in the along-track direction (see e.g. Table 7 in Sect. 4 of this paper).

For observing the non-gravitational accelerations, an accelerometer would ideally be located in the center of mass (COM) of the satellite, which is almost perfectly the case for the CHAMP and GRACE satellites (GSFC 2002; Reigber et al. 1999). Equivalently, when using CM accelerometer observations, the center of the gradiometer would then in the ideal case coincide with the satellite's center of mass. This is however not the case leading to additional terms in the accelerometer observation equations, namely a term associated with the local satellite gravity gradients, and terms due to centrifugal and angular accelerations. By taking the proper combination of accelerometer pairs, these terms can almost be perfectly eliminated, making the use of CM accelerometer observations in precise orbit determinations rather straightforward. For a three-axes gradiometer consisting of three-axes accelerometers, it is possible to make 3 CM combinations for each direction. Thus, 9 CM accelerometer biases and scale factors can then be estimated, whereas a total of 3×6 or 18 individual accelerometer biases and scale factors can be identified. The estimation of these 9 CM biases and scale factors can be considered as a partial, be it very valuable, calibration of the accelerometers.

The objective of the work to be described in the remainder of this paper is to explore also the possibility of estimating biases and scale factors for all six individual accelerometers. It has to be noted that such an estimation is not the baseline method for the calibration, but should be seen in support of the methods as outlined by Bouman et al. (2004). However, a proper calibration of the GOCE accelerometers is critical for mission success. The method outlined in this paper will function as an offline tool to validate the calibration applied to the observations that will be provided by the GOCE project to the scientific community.

After introducing the required observation types (Sect. 2), the adopted treatment of the accelerometer observations will be described and the method of estimating calibration parameters for the CM and individual accelerometer observations (Sect. 3). Both the methods for estimating calibration parameters for individual and CM accelerometer observations will be applied to simulated test data from an End-to-End simulator (Catastini et al. 2006; Visser 2007a, Sect. 4). The effect of gravity field model errors will be assessed, together with possibilities to mitigate this effect. Finally, conclusions will be drawn about the feasibility of the proposed method (Sect. 5).

2 Observations

In principle, the GOCE orbit and accelerometer calibration parameters are to be determined from the GPS SST observations for the method outlined in this paper. A two-step approach will be adopted, where in the first step a kinematic precise orbit determination will take place. The resulting time series of satellite positions will be used in the second step as pseudo-observations for a combined estimation of orbit parameters, accelerometer calibration parameters and, if so required, also gravity field coefficients or empirical accelerations (Visser et al. 2001, 2006; Bock et al. 2007). For this paper, only the second step will be considered and it is assumed that time series of Cartesian x, y and z coordinates in an earth-centered, earth-fixed (ECF) coordinate frame are available together with rotation parameters that establish the connection between the ECF and J2000 earth-centered pseudo-inertial reference frame (Montenbruck and Gill 2000). It has to be noted that the three-dimensional orbit precision requirement for GOCE is at the few cm level. An assessment has been made of the impact of random orbit errors at the few cm level on accelerometer bias and scale factor estimates.

The accelerometer observations are provided as time series in the gradiometer reference frame (GRF, Fig. 1). The orientation of this GRF in the J2000 reference frame is provided by quaternions derived from star tracker observations. It is crucial to accurately model the accelerometer observations and possibly apply corrections before using them in precise orbit computations. For all accelerometers, the linear non-gravitational accelerations $\mathbf{d}$ are the same and are modeled as (cf. Eqs. (7.2.1) and (7.2.2) in ESA 1999):

$$\mathbf{d} = \mathbf{S}_i^{-1}(\mathbf{a}_{\text{obs},i} - \mathbf{b}_i - \epsilon_i) - (\Gamma + \mathbf{R})\mathbf{x_i} \qquad (2)$$

where $\mathbf{S}_i$ represents the 3×3 diagonal scale factor matrix, and $\mathbf{a}_{\text{obs},i}$, $\mathbf{b}_i$, ϵ_i respectively the three-dimensional vectors of observations, biases and observations errors, all for accelerometer i ($i = 1, \ldots, 6$). The gravity gradient tensor and matrix with rotational terms are represented by Γ and $\mathbf{R}$. Finally, the offset of accelerometer i with respect to the satellite's center of mass is indicated by $\mathbf{x}_i$, cf. Visser (2007b).

It has to be noted that Eq. (2) does not include effects due to misalignments, non-orthogonalities, couplings and quadratic terms. However, the requirement for the combined effect of non-orthogonalities and couplings between the accelerometer axes is smaller than 1.3×10^{-4} rad (Cesare and Catastini 2005). In addition, the requirement for GOCE is that the misalignments are smaller than 0.001 rad (Cesare 2005), which means that their contribution to a possible scale factor is of the order (or smaller than) 0.001. Therefore, misalignments, non-orthogonalities, couplings and quadratic terms will not be taken into account in the modeling of the accelerometer observations (Sect. 3).

3 Methodology

The estimation process is based on a conventional dynamic orbit determination, where the observation equations for the time series of x, y and z satellite position coordinates are obtained by numerical integration of the variational equations and solved by a Bayesian weighted least-squares method (Montenbruck and Gill 2000). For all computations described in this paper, a uniform weight was applied to observed satellite position coordinates.

3.1 Calibration by precise orbit determination

Nominally, the CM observations of sensitive axes are used to represent the non-gravitational accelerations, equivalent to the use of accelerometer observations in CHAMP- and GRACE-based orbit and gravity field determinations (Tapley et al. 2005; Reigber et al. 2003). For GOCE, this means the pair 1 and 4 for the X axis, 2 and 5 for the Y axis, and 3 and 6 for the Z axis (Fig. 1). A bench mark computation has been conducted where calibration parameters are estimated for these CM observations (see top of Table 2 in Sect. 4). However, as outlined in Sect. 1, nine different CM combinations can be made, three combinations for each direction. Therefore, three additional series of orbit determinations have been done as well to estimate calibration parameters for all these nine combinations (see middle parts and bottom of Table 2). However, the primary objective is to investigate whether calibration parameters for observations taken by the individual accelerometers can be reliably estimated by, in this case six, separate precise dynamic orbit determinations as well, i.e. one for each accelerometer. An assessment of the need for correcting the accelerometers for gravity gradient and rotational terms has been included in the investigations.

Both for the CM and individual accelerometer observations, biases, accelerometer drifts and scale factors can be estimated. Analysis of simulated test data (Sect. 4) has indicated that the currently anticipated behavior of the accelerometers outside the measurement bandwidth display a slowly changing drift (cf. Fig. 3 in Visser 2007b). Therefore, the accelerometer bias is considered to be changing in time. The bias vector $\mathbf{b}_i$ in Eq. (2) is modeled as:

$$\mathbf{b}_i = \mathbf{b}_{i,0} + \mathbf{b}_{i,t} t \tag{3}$$

where t represents time, and $\mathbf{b}_{i,0}$ and $\mathbf{b}_{i,t}$ represent the biases at the starting time of the orbital arcs and the accelerometer drifts, respectively.

3.2 Correcting the accelerometer observations

Each accelerometer experiences different accelerations due to the local satellite gravity gradient and due to rotational

effects (angular accelerations and centrifugal terms). First of all, the location of each individual accelerometer has to be defined (Fig. 1):

$$\begin{aligned}
\mathbf{x_1}^T &= (o_x + L_x/2, o_y, o_z) \\
\mathbf{x_2}^T &= (o_x, o_y + L_y/2, o_z) \\
\mathbf{x_3}^T &= (o_x, o_y, o_z + L_z/2) \\
\mathbf{x_4}^T &= (o_x - L_x/2, o_y, o_z) \\
\mathbf{x_5}^T &= (o_x, o_y - L_y/2, o_z) \\
\mathbf{x_6}^T &= (o_x, o_y, o_z - L_z/2)
\end{aligned} \tag{4}$$

where, L_x, L_y, L_z are the gradiometer arm lengths along the X, Y and Z axes, and $\mathbf{o}^T = (o_x, o_y, o_z)$ represents the offset of the center of the gradiometer instrument with respect to the satellite center of mass. Second, the gravity gradients can be derived from an a priori gravity field model. Finally, rotational terms need to be accounted for. The star tracker observations provide the orientation of the gradiometer reference frame in the J2000 inertial reference frame and are used, together with orbital information (position and velocity), to derive the yaw, pitch and roll angles (ϕ_i, $i = 1, 3$) around the axes of the gradiometer reference frame. It has to be noted that the axes of the selected star tracker (GOCE will have three, with two always providing observations) are not aligned with those of the gradiometer reference frame. In fact, a rotation of 60° around the X axis has to be applied to the observations for the selected star tracker to obtain rotational values in the GRF. The relatively large star tracker observation errors around the bore sight are thus spread over more axes. This means that the results presented in this paper might be considered pessimistic. In reality, it might be possible to combine observations taken by the two active star trackers on-board of GOCE. These star trackers have different orientations, thereby opening the possibility of reducing errors around the bore sight direction. First and second time derivatives of the rotation angles are obtained by using a moving time window of certain width over the time series of these angles and fitting second-order polynomials:

$$\phi_i = \phi_0 + \dot{\phi}t + \ddot{\phi}t^2 \tag{5}$$

where ϕ_0 is the initial condition of each estimated polynomial, and the coefficients $\dot{\phi}$ and $\ddot{\phi}$ represent the angular rotation rate (from which the centrifugal accelerations can be derived) and angular acceleration, respectively. Depending on the noise characteristics of the star tracker, a longer or shorter time window might be required (Visser 2007b).

4 Results

Use has been made of simulated GOCE observations (April 2008) from a comprehensive End-to-End simulator

(Catastini et al. 2006; Visser 2007a). The so-called Acceptance Review 2 (AR2) data set was used, which was generated in March 2006 for testing the so-called Version 2 of the High-level Processing Facility (HPF) implementation (Koop et al. 2006). The End-to-End simulator takes into account all anticipated error sources, including star tracker noise and biases, and accelerometer biases, quadratic terms, non-orthogonalities, scale factors, misalignments and colored noise. As noted before, misalignments, quadratic terms and non-orthogonalities are considered to be negligibly small in accordance with GOCE requirements. The satellite environment is modeled in great detail in the End-the-End simulator, including the EGM96 gravity field model part complete to degree and order 200 for the orbit perturbations (Lemoine et al. 1988) and non-gravitational forces. The star-tracker observation errors are typically of the order of $20''$ (arcsec) for the more precise rotation axes and up to $50''$ for the bore sight axis (cf. Fig. 3 in Visser 2007a) and are provided with a 0.5 s time interval. A time window of 100 s was used to derive the angular rotation rates and accelerations (Eq. (5), see also Sect. 3.1 in Visser 2007b). It has to be noted that the true values for the accelerometer scale factors and biases as used in the End-to-End simulator were not provided. However, it was specified that for these data, the deviations of the scale factors from 1 are less than 0.001 (0.1%). The End-to-End data were generated with completely independent software. The tests described in this paper can thus be considered as a software validation as well.

The effect of gravity field model errors was also assessed. Experiments included gravity field model error simulations complete to degree and order 50 ("50 × 50") and 200 ("200 × 200"), respectively. First, it was investigated if stable accelerometer calibration parameters could be estimated, together with either gravity field coefficients complete to degree and order 50 or 80 using an End-to-End simulator data set of 10 or 20 days (11–20 or 3–22 April 2008). It has to be noted that no regularization was applied in all cases, i.e. no constraints were applied for estimating gravity field coefficients. In addition, it was investigated how well gravity field model error could be absorbed by co-estimating empirical accelerations. The NASA Goddard Space Flight Center GEODYN software was used for computing the observation and associated normal equations (Pavlis et al. 2006).

4.1 Calibration by precise orbit determination

Estimations of calibration parameters were conducted for all combinations of CM accelerometer observations (Sect. 4.1.1) and for all individual accelerometer observations (Sect. 4.1.2). Use was made of 24-h or daily arcs and for each individual accelerometer or CM combination a separate estimation was done. Unless otherwise stated, the estimated parameters are the satellite begin position and velocity, a bias

and scale factor per accelerometer or common-mode axis and a bias drift for the X axis, equivalent to a total of 13 parameters per day. In case of gravity field model error, gravity field coefficients or resonant 1 cycle per orbital revolution (cpr) empirical accelerations can be estimated as well (Table 1). When estimating gravity field coefficients, normal equations are still set up for daily arcs, but the gravity field part will be combined for the entire data period. In addition, tests have been done where empirical accelerations are estimated once per 1.5 h (about 1 orbital revolution), once per hour, and once per half hour.

4.1.1 CM accelerometer observations

First, reference one-day estimation runs were conducted from error-free time series of x, y and z satellite positions with a time interval of 10 s. Use was made of an error-free gravity field model (for the simulated End-to-End orbit, the EGM96 model was truncated at degree 200) and CM accelerometer observations for the sensitive axes. It was found that the inclusion of accelerometer drifts for only the X direction in the estimation process, together with accelerometer biases and scale factors, resulted in the best orbit fit and scale factor values very close to 1, except for the X axis (Table 2). The remaining orbit residuals are of the order of 2 cm, which can be explained by the modeling of the low-frequency observation noise. For example, the effect of not taking into account the accelerometer drift in the X axis already causes the orbit fit to deteriorate to about 18 cm (Table 2). At the low frequencies outside the MB, the accelerometer observation errors are predicted to be proportional to the inverse of the frequency and relatively slowly changing with time (cf. Fig. 2 in Catastini et al. 2006), causing a building up of orbit error.

It can be observed that the scale factor for the X axis deviates by about 0.3 from 1 when an accelerometer drift for the X axis is estimated (the deviation is about 0.6 when no such drift is estimated). This large deviation can be explained by the DFC, which leaves only a small signal for this direction (especially compared to the accelerometer drift) making it difficult to determine an accurate scale factor. Small modeling errors, such as caused by the fact that the center of the gradiometer does not coincide with the COM of the satellite, then lead to large scale factor deviations from 1. It can also be observed that for all CM combinations, very similar results are obtained for the calibration parameters and orbit fits. It can thus be concluded that observations taken by sensitive and les-sensitive axes lead to comparable results. It was found as well that almost identical scale factors for the Y direction were obtained when the scale factor for the X direction was put to zero or frozen at one and not estimated. It has to be noted that fixing the scale factor for the X axis to one thus hardly affects the results. By putting the scale factor for the X axis equal to one, no use is made of

Table 1 Overview of estimated parameters and their a priori values and constraints

Nominal		
	Orbit parameters	Begin position and velocity for 24-h batches (6)
	Calibration parameters	For each accelerometer: one bias and scale factor per 24 h and per axis, one bias drift parameter for the X axis per 24 h (7). However, for many cases, the X axis scale factor is constrained to 0.
Optional		
	Gravity field parameters	Spherical harmonic coefficients complete to degree and order 50 (2,597) or 80 (6,557) for a 10-day or 20-day period
	Empirical accelerations	Radial and cross-track 1-cpr accelerations:
		- per 1.5 h (64)
		- per 1.0 h (96)
		- per 0.5 h (192)
Initial conditions		
	Orbit parameters	Begin position & velocity from precise orbit determination
	Calibration parameters	Accelerometer biases and drifts = 0
		Scale factors = 1
	Gravity field parameters	From a priori gravity field model
	Empirical accelerations	A priori value = 0
Weight of observations		
	Satellite x, y, z positions	$\sigma = 10$ cm
A priori constraints		
	Orbit parameters	None
	Calibration parameters	Only for scale factors: $\sigma_{\mathrm{apriori}} = 1.0$
	Gravity field parameters	None
	Empirical accelerations	$\sigma_{\mathrm{apriori}} = 1.0 \times 10^{-6}$ m/s^2

For each accelerometer or for each common-mode, separate daily estimation runs are made. The numbers between brackets specify the amount of estimated parameters for these separate daily runs

the a priori knowledge that for the accelerometer observations provided by the End-to-End simulator this scale factor is very close to one. Therefore, results with a value of zero for the X axis scale factor can be considered to be the worst case. The scale factor for the Z direction then changed by less than 0.003. Finally, orbit errors at the 2 cm level hardly affect the scale factor estimates for the Y and Z axes, whereas the change for the X direction is of the order of 0.01, much below the deviation from 1. Therefore, the effect of orbit error will no longer be taken into consideration.

The CM accelerometer observations are obtained by taking the mean of observations taken by two accelerometers on one axis. Nominally, this point coincides with the center of the gradiometer. This center does not coincide with the COM of the satellite. Ideally, the non-gravitational accelerations would be known for the COM. The correction for this COM offset $\mathbf{a}_{\mathrm{com}}$ can be obtained from the accelerometer observations themselves:

$$\mathbf{a}_{\mathrm{com}} = \frac{o_x}{2a}\,(\mathbf{a}_1 - \mathbf{a}_4) + \frac{o_y}{2a}\,(\mathbf{a}_2 - \mathbf{a}_5) + \frac{o_z}{2a}\,(\mathbf{a}_3 - \mathbf{a}_6) \quad (6)$$

where $\mathbf{a_i}$ ($i = 1, \ldots, 6$) are the observations taken along all three axes by the individual accelerometers. As an example, let us assume that the first accelerometer is in the center of

mass. In that case, o_x is equal to half the arm length or a and the correction is equal to $\frac{1}{2}(\mathbf{a}_1 - \mathbf{a}_4)$. Adding this correction to the CM then leads to $\frac{1}{2}(\mathbf{a}_1 + \mathbf{a}_4) + \frac{1}{2}(\mathbf{a}_1 - \mathbf{a}_4) = \mathbf{a}_1$, which are the observations of the accelerometer that is located at the center of mass.

When taking into account the COM correction ($b = 3.45$ cm for the End-to-End data, Fig. 1) according to Eq. (6), a significant improvement is obtained for the X axis scale factor estimates: the deviation from 1 is reduced from about 0.3 to 0.08. This is however, still much higher than for the other two directions leading to the conclusion that it will be difficult to obtain reliable scale factor estimates for the X direction by precise orbit determination (this is also reflected by the formal errors, which will be discussed in Sect. 4.1.3). The fact remains that the signal is small for this direction because of the DFC. It has to be remarked that when correcting for the COM offset by using Eq. (6), all six accelerometers might make a contribution (in case of offsets along all three axes). This has to be taken into consideration when interpreting the estimated biases, drifts and scale factors.

Moreover, it might be argued that it is fair to anticipate that the estimation of scale factors for the accelerometer X axis results in anomalous values. The DFC is fed by the common-mode of a sensitive pair of accelerometers. In the

Table 2 Estimated one-day accelerometer scale factors, biases (nm/s^2) and drifts (nm/s^2 per day) for the CM accelerometer observations for different parameterizations by precise orbit determination for 11 April 2008 (top)

Acc.	SF X	SF Y	SF Z	Orbit (cm)	Bias X	Bias Y	Bias Z	Drift X
Common-mode sensitive axes (1&4/2&5/3&6)								
No drift	1.610	0.999	0.989	17.66	127.39	−57.69	−259.19	0.0000
Drift	0.731	0.999	0.990	2.02	130.44	20.09	65.98	5.0740
Drift[a]	0.923	0.999	0.991	2.02	133.63	931.37	72.36	4.6101
Drift[c]	–	0.999	0.988	1.99	128.94	20.98	64.94	5.0782
Drift[d]	1.000	0.999	0.990	2.04	131.00	19.76	66.37	5.8712
Common-mode pair 1&4								
Drift	0.738	0.999	0.988	2.06	130.15	−18, 170.40	80.65	5.9367
Drift[a]	0.927	0.999	0.988	2.06	133.34	−17, 257.20	87.02	5.4712
Drift[a,b]	0.921	0.999	0.989	2.87	133.31	−17, 257.00	87.22	5.4733
Common-mode pair 2&5								
Drift	0.801	0.999	0.990	1.99	41.38	18.40	−14, 125.90	−1.6269
Drift[a]	0.929	0.999	0.991	1.98	30.23	929.64	−14, 132.00	−3.1366
Drift[a,b]	0.924	0.999	0.991	2.82	30.70	929.55	−14, 135.90	−3.0992
Common-mode pair 3&6								
Drift	0.763	0.999	0.991	2.02	−149.65	−11, 851.20	61.20	−7.6218
Drift[a]	0.900	0.999	0.992	2.02	−197.11	−10, 938.60	66.89	−10.3213
Drift[a,b]	0.887	0.999	0.992	2.84	−192.58	−10, 938.50	67.14	−10.1119

The fit of the time series of orbit x, y and z coordinates is included as well. SF X, Y and Z denote the scale factors for the three accelerometer axes, or the diagonal of the scale factor matrix **S** in Eq. (2). The mean of the CM observations (nm/s^2) is included as reference (bottom)

[a] COM offset correction applied (Eq. (6))
[b] Gaussian orbit errors ($\sigma_{orb}= 2$ cm)
[c] Scale factor for X axis equal to zero
[d] Scale factor for X axis equal to one

Pair	Mean X	Mean Y	Mean Z
1&4	−4.80	17,913.72	327.79
2&5	111.88	−297.31	14,664.69
3&6	373.47	11,583.12	343.94

hypothetical case that the DFC is perfect, the satellite will no longer experience an acceleration along the X axis except for the CM observation error. This thus leads to a situation where the satellite experiences an acceleration signal along the X axis equal to the CM observation error. On top of this, the satellite will experience an acceleration due to thruster noise. It might thus be concluded that scaling of the X-axis components by orbital analysis is conceptually impossible in the case of a perfect DFC. Only in case of high thruster noise levels (much above the accelerometer observation noise levels), an accurate scaling might be possible.

The values for the biases for the CM combinations are included in Table 2 as well. Because of the simulated $1/f$ noise, the biases will not be the same for different days (see also Table 6). It has to be noted that for the gradiometer observations, the determination of accelerometer bias and bias drift values is not as important as the determination of the scale factors, considering the gradiometer bandwidth of 0.005–0.1 Hz (Visser 2007b). It can be observed that the drifts are of

the order of 1–10 nm/s^2 per day and biases are of the order of 10^{-7} to 10^{-5} m/s^2, depending on whether COM corrections are applied or not. Although the biases are not constant in the simulated data set, an assessment can be made of how well the estimated biases represent the mean observation error for the daily arcs. This can be done by comparing the differences between the estimated biases for different CM combinations with the difference between the mean of the CM observations. For example, the mean of the CM observations for pair 1&4 and pair 2&5 is equal to −4.80 and 111.88 nm/s^2 for the X axis, a difference of 107.08 nm/s^2 (bottom of Table 2). The difference between the associated biases is equal to 133.31 − 30.70 = 102.61 nm/s^2, when applying the COM offset and estimating an accelerometer drift. The discrepancy is thus only 4.47 nm/s^2. For the Y and Z axis, the discrepancies are typically a few orders of magnitude higher. Although the estimated bias and drift values will be provided for all cases, the focus in the remainder of this paper will be on the scale factors.

4.1.2 Individual accelerometer observations

In consecutive series, the raw accelerometer observations were used. The accelerometer observations corrected for rotational terms as derived from the star tracker observations (Eq. (5), indicated by "ROT"), and the accelerometer observations corrected for both rotational and gravity gradient terms using the EGM96 gravity field model truncated at degree and order 20 (indicated by "ROT+GG"). In addition, the estimated parameters excluded or included accelerometer X-axis accelerometer drifts. It was found that the estimated scale factors for the Y and Z directions are closest to 1 when applying both the rotational and gravity gradient corrections and when estimating accelerometer drifts for the X axes: all Y and Z scale factor values deviate less than 0.01 from 1, except for one value deviating by 0.015 (accelerometer 5, Table 3 middle). The estimation of scale factors for the X direction again turned out to be rather unreliable. The deviations from 1 are larger than for the cases where the CM observations were used (Sect. 4.1.1). In general, the deviations from 1 are also larger for the Y and Z directions when comparing the scale factor estimates for the individual accelerometer with the CM observations. This can be explained by the fact that the individual accelerometer observations needed to be corrected for rotational terms derived from the relatively noisy star tracker observations. Finally, the effect of not estimating scale factors for the X direction led to changes in the scale factors for the Y direction that are less than 0.001, and less than 0.006 for the Z direction.

The accelerometer biases are of the order of 10^{-7} to 10^{-5} m/s^2 (Table 3 top). In addition, it was found that the accelerometer drifts are of the order of 10^{-8} m/s^2 per day. The Root-Mean-Square (RMS) about mean of the observed nongravitational accelerations are of the order of 5×10^{-8}, 10^{-6} and 4×10^{-7} m/s^2 for the X, Y and Z directions, respectively. The signal in the X direction is rather noisy, whereas the signals for the Y and Z direction are dominated by 1 and 2 cpr terms and thus more systematic. The integrated effect of the accelerometer drift along the X axis is of the order of a few dm after one day, which dominates the effect of the remaining accelerometer noise. Moreover, accelerometer observation errors accumulate much more rapidly in terms of position in the predominantly along-track X direction than in the Y and Z directions. Therefore, it can be argued again that the scaling in the X direction is much more unreliable than in the other two directions in case the behavior outside the measurement bandwidth (0.005–0.1 Hz) at especially the longer wavelength is as predicted by the End-to-End simulator (again, see also Sect. 4.1.3 for the formal errors).

In the correction of the observations of the individual accelerometers for rotational terms, use is made of an averaging window (Eq. 5). Use was made of the star tracker quaternions to serve as an independent set of observations to derive the rotational terms. Also, for GOCE use can be made of less noisy attitude quaternions. By taking appropriate combinations of the DM accelerometer observations, angular accelerations can be obtained that are integrated in time and merged optimally with the star tracker observations through a Kalman filter in order to obtain orientation angles with a very low noise level (Cesare and Catastini 2005). It is anticipated that shorter averaging windows can then be used for deriving the rotational terms, leading to smaller modeling errors due to smoothing of the underlying signal. It has, however, to be realized that the same accelerometer observations are then used twice, once for deriving the rotational corrections and once for representing the non-gravitational accelerations in the orbit determination, whereas only for the latter part calibration parameters are estimated. Thus it might be said that "one is biting its own tail" when using the latter quaternions and the calibration becomes more a consistency check.

In case the accelerometers would not be properly calibrated (the a priori scale factors should have a precision better than 10^{-4} in the gradiometer measurement bandwidth of 5–100 mHz for meeting the gravity gradient precision requirements), an iterative procedure would be required because of the improperly derived rotational terms (the proper working of star trackers has been proved already by missions like CHAMP and GRACE). When using the less noisy quaternions, the resulting scale factors were found to be even closer to 1: the deviation is in all cases significantly below 0.01 for the Y and Z directions (Table 3, bottom). Almost identical results were obtained for 25 and 100 s averaging windows, showing that the effect of smoothing due to an averaging window of 100 s is limited.

Finally, a 10-day period was analyzed to test the consistency of the estimations for different days. This resulted in scale factors for the Y and Z directions that are consistent at a level better than 0.01 in the absence of gravity field model error (Table 5, top). It has to be noted that for results included in Table 5 and also Tables 6, 7, 8, 9, the accelerometer observations were corrected for rotational and gravity gradient terms. Also, the scale factor for the accelerometer X axes was put to zero, unless when indicated that this was not the case. The RMS-about mean for the estimated accelerometer biases is relatively large for the Y and Z directions 28–225 nm/s^2), and especially low for the X direction when the scale factor for this direction is fixed (5 nm/s^2, Table 6, top). The values found for the accelerometer mean drift and RMS-about-mean are of the order of 5 nm/s^2 per day, indicating that the drift is not constant and slowly changing all the time.

The differences between the biases of different accelerometers can again be compared with the differences in the mean of the observations by the individual accelerometers (as was done for the CM, see Sect. 4.1.1). The daily means of the individual accelerometer observations are included in Table 4 together with their RMS-about mean for the 10-day

Table 3 Estimated accelerometer one-day biases (nm/s^2), drifts (nm/s^2/day), and scale factors for the individual accelerometers (11 April 2008)

Quaternions from star trackers, 100 s averaging window

Acc	Bias X	Bias Y	Bias Z	Drift X	Bias X	Bias Y	Bias Z	Drift X
					ROT			
1	180.84	180.84	−37.39	0.00	−317.85	−31, 392.50	21.93	0.00
2	43.78	43.78	−26, 402.00	0.00	85.47	677.55	−27, 611.30	0.00
3	57.51	57.51	−688.39	0.00	67.93	7, 085.70	−331.31	0.00
4	165.07	165.07	172.99	0.00	−71.29	−4, 952.97	198.80	0.00
5	77.55	77.55	−3, 165.73	0.00	93.39	−665.26	−2, 549.95	0.00
6	−126.57	−126.57	731.96	0.00	−96.46	−29, 482.20	455.16	0.00
ROT+GG					ROT+GG, Drift			
1	179.97	−31, 103.90	77.45	0.00	113.25	−31, 222.50	84.23	9.59
2	83.71	159.20	−24, 893.50	0.00	113.31	166.14	−24, 883.50	2.96
3	56.10	6, 840.06	154.59	0.00	76.68	6, 841.11	155.16	1.66
4	166.83	−4, 918.01	242.83	0.00	142.80	−4, 899.62	246.18	3.07
5	−87.38	−168.40	−3, 141.09	0.00	125.92	−65.23	−3, 317.86	5.60
6	−122.76	−30, 398.10	139.89	0.00	−1.57	−30, 378.20	141.59	2.02
ROT+GG, Drift								
1	128.31	−31, 196.20	83.49	7.44				
2	129.26	169.81	−24, 878.20	4.55				
3	128.92	6, 843.74	156.49	5.87				
4	129.31	−4, 889.50	247.36	4.79				
5	129.24	−64.01	−3, 322.39	5.66				
6	129.50	−30, 357.30	142.45	4.20				

Acc.	SF X	SF Y	SF Z	Orbit (cm)	SF X	SF Y	SF Z	Orbit (cm)
					ROT			
1	−1.260	1.003	0.885	4.40	−1.277	1.000	0.922	2.58
2	0.622	0.991	1.048	13.17	0.471	0.988	1.093	14.82
3	0.225	1.033	1.008	8.92	0.226	1.031	1.005	8.68
4	0.793	0.998	0.999	2.03	0.799	0.997	1.008	2.23
5	0.674	1.000	0.925	11.39	1.621	1.008	0.810	15.41
6	0.637	0.962	0.970	6.08	0.637	0.964	0.967	5.84
ROT+GG					ROT+GG, Drift			
1	−1.277	0.992	1.019	2.66	0.372	0.995	0.993	1.46
2	0.298	0.994	0.993	1.43	0.104	0.994	0.993	1.26
3	0.225	0.993	1.005	1.24	0.162	0.993	1.006	1.22
4	0.815	0.994	0.991	1.43	0.293	0.993	0.999	1.09
5	3.327	0.997	0.904	10.80	0.051	0.992	1.013	1.34
6	0.621	0.995	0.993	1.38	0.323	0.994	0.997	1.20
ROT+GG, Drift								
1	−	0.994	0.999	1.50				
2	−	0.994	0.992	1.27				
3	−	0.993	1.009	1.21				
4	−	0.994	1.004	1.10				
5	−	0.992	1.015	1.33				
6	−	0.994	1.001	1.27				

Table 3 continued

Quaternions from combination of star trackers and gradiometer								
Acc.	SF X	SF Y	SF Z	Orbit (cm)	SF X	SF Y	SF Z	Orbit (cm)
ROT+GG, Drift					ROT+GG, Drift			
100 s averaging window					25 s averaging window			
1	0.301	0.996	0.993	1.71	0.312	0.994	0.993	1.48
2	0.004	0.993	1.003	1.25	0.057	0.993	1.003	1.26
3	0.146	0.991	1.000	1.57	0.148	0.993	0.999	1.26
4	0.357	0.991	0.997	0.97	0.340	0.993	0.998	1.08
5	0.095	0.993	1.000	1.41	0.045	0.993	1.000	1.28
6	0.315	0.996	1.000	1.03	0.297	0.994	1.001	1.16
1	–	0.995	0.998	1.71	–	0.994	0.997	1.49
2	–	0.993	1.004	1.24	–	0.993	1.004	1.25
3	–	0.991	1.002	1.56	–	0.992	1.001	1.25
4	–	0.991	1.001	1.02	–	0.993	1.003	1.11
5	–	0.993	1.006	1.40	–	0.993	1.001	1.27
6	–	0.996	1.006	1.10	–	0.994	1.006	1.21

The fit of the time series of satellite x, y, z positions is included as well. ROT and GG indicate that the accelerometers have been corrected for respectively, rotational and/or gravity gradient terms

period. This RMS-about-mean is between 9 and 127 nm/s^2, of the same order of magnitudes of the RMS-about-mean of the estimated bias parameters. It can also be observed that the values in Tables 4 and 6 have a consistency level of the order of a few 100 nm/s^2 or better.

The orbital fit for the 10-day period is higher than for the one-day tests: about 4 cm compared to 1.5 cm. It was found that the fit varies between 1 and 6 cm for the individual days. The simulated low-frequency accelerometer observation noise manifests itself as a slowly changing drift resulting in different patterns for different days and causing different orbit determination error levels, i.e. for certain days the along-track accelerometer drift is better able to absorb dynamic model errors due to this low-frequency noise than for other days. However, it was shown before that an orbit error level of the order of a few cm hardly affects the scale factor estimates (cf. Table 2). Again, ignoring the scale factors for the X direction led to small changes for the other scale factors:

Table 4 Daily means and their RMS-about-mean (nm/s^2) of the individual accelerometer observations for 11–20 April 2008

Acc.	Mean X	Mean Y	Mean Z
1	-11.54 ± 33.84	$32, 248.99 \pm 126.52$	226.02 ± 36.32
2	224.19 ± 37.23	408.94 ± 33.61	$25, 604.09 \pm 110.92$
3	392.68 ± 22.86	$-6, 138.66 \pm 55.93$	240.51 ± 27.00
4	3.68 ± 34.01	$5, 662.95 \pm 99.48$	82.86 ± 28.28
5	53.97 ± 9.07	830.69 ± 75.11	$3, 455.03 \pm 118.31$
6	392.27 ± 26.29	$31, 081.51 \pm 78.87$	299.01 ± 61.32

less than 0.001 for the Y direction and 0.002–0.013 for the Z direction.

4.1.3 Formal errors

For selected cases, formal errors and correlations between the estimated parameters were derived from the normal equations (Table 7). It was found that especially the bias and scale factor for the Y axis are heavily correlated (>0.99 for all cases). For cases where the X axis scale factor is estimated, the correlations between the bias, drift and scale factor were heavily correlated as well (also >0.99). The effect of the additional high correlations for these cases is reflected by the relatively large formal errors. It can be observed that when estimating the scale factor for the X axis, its formal error is a few orders of magnitude larger than for the other two axes, corroborating the assumption that this scale factor is hardly observable because of the small signal in the X direction. Also, it can be observed that the formal error for the Y direction is smaller than for the Z direction, which is consistent with the results presented in the previous sections. The formal error for the bias in the X direction is much smaller than for the Y and Z directions for all cases. This is in accordance with the results obtained so far as well.

4.2 Effect of gravity field model error

The results presented so far are based on an error-free modeling of the gravitational forces in the precise orbit determination (Sect. 4.1). Accelerometer calibration parameters

Table 5 Estimated daily scale factor values and their RMS-about-mean for the individual accelerometers for cases excluding and including gravity field model errors, and for cases excluding and including the co-estimation of gravity field SH coefficients

Acc.	SF X	SF Y	SF Z	Orbit (cm)
10 1-day arcs, no gravity error, estimation of cal. parameters only				
1*	0.087 ± 0.292	0.992 ± 0.0017	0.999 ± 0.0085	4.22
2*	0.319 ± 0.299	0.992 ± 0.0013	0.996 ± 0.0064	3.99
3*	0.299 ± 0.378	0.991 ± 0.0015	1.003 ± 0.0073	4.03
4*	0.195 ± 0.262	0.991 ± 0.0013	0.999 ± 0.0063	3.92
5*	0.285 ± 0.272	0.990 ± 0.0015	1.003 ± 0.0107	4.06
6*	0.340 ± 0.294	0.992 ± 0.0015	0.997 ± 0.0051	4.03
1	–	0.992 ± 0.0015	1.001 ± 0.0056	4.22
2	–	0.992 ± 0.0013	0.994 ± 0.0055	3.99
3	–	0.991 ± 0.0014	1.010 ± 0.0055	4.03
4	–	0.991 ± 0.0013	1.002 ± 0.0056	3.92
5	–	0.990 ± 0.0011	1.014 ± 0.0053	4.06
6	–	0.992 ± 0.0014	1.001 ± 0.0053	4.03
10 1-day arcs, clone50, estimation of calibration parameters only				
1	–	0.992 ± 0.011	1.001 ± 0.010	7.00
2	–	0.992 ± 0.011	0.994 ± 0.010	6.86
3	–	0.991 ± 0.011	1.009 ± 0.010	6.89
4	–	0.990 ± 0.011	1.002 ± 0.011	6.82
5	–	0.990 ± 0.011	1.014 ± 0.010	6.90
6	–	0.991 ± 0.011	1.000 ± 0.009	6.87
10 1-day arcs, clone50, co-estimation of 50 × 50 SH coefficients				
1	–	0.991 ± 0.021	0.994 ± 0.062	1.54
2	–	0.995 ± 0.023	0.994 ± 0.064	0.82
3	–	0.992 ± 0.017	1.003 ± 0.051	0.84
4	–	0.989 ± 0.025	0.993 ± 0.053	0.81
5	–	0.987 ± 0.022	1.008 ± 0.065	0.94
6	–	0.994 ± 0.018	1.006 ± 0.073	1.19
10 1-day arcs, clone200, estimation of calibration parameters only				
1	–	0.986 ± 0.014	0.999 ± 0.077	16.19
2	–	0.986 ± 0.014	0.993 ± 0.075	16.03
3	–	0.985 ± 0.014	1.008 ± 0.076	16.19
4	–	0.985 ± 0.014	1.001 ± 0.075	16.00
5	–	0.985 ± 0.014	1.012 ± 0.076	16.15
6	–	0.986 ± 0.014	0.999 ± 0.076	16.09
10 1-day arcs, clone200, co-estimation of 80 × 80 SH coefficients				
1	–	0.996 ± 0.091	1.097 ± 0.416	2.98
2	–	1.004 ± 0.091	1.094 ± 0.383	2.78
3	–	0.999 ± 0.093	1.108 ± 0.408	2.76
4	–	0.996 ± 0.089	1.098 ± 0.402	2.76
5	–	0.992 ± 0.094	1.113 ± 0.402	2.76
6	–	1.001 ± 0.094	1.109 ± 0.398	3.02
20 1-day arcs, clone200, co-estimation of 80 × 80 SH coefficients				
1	–	1.0116 ± 0.0991	1.064 ± 0.511	9.08
2	–	1.0152 ± 0.0991	1.064 ± 0.504	8.99
3	–	1.0108 ± 0.0981	1.073 ± 0.515	9.02
4	–	1.0118 ± 0.0991	1.063 ± 0.508	8.97
5	–	1.0088 ± 0.1007	1.079 ± 0.485	9.00
6	–	1.0147 ± 0.0987	1.071 ± 0.510	9.09

* Scale factor for X axis estimated

Table 6 Estimated biases (nm/s²) and drifts (nm/s² per day) and their RMS-about-mean for the individual accelerometers for cases excluding and including gravity field model errors, and for cases excluding and including the co-estimation of gravity field SH coefficients

Acc.	Bias X	Bias Y	Bias Z	Drift X
10 1-day arcs, no gravity error, estimation of cal. parameters only				
1*	138.65 ± 13.29	$-31,346.34 \pm 99.12$	170.70 ± 52.73	4.5507 ± 4.7267
2*	65.55 ± 74.61	223.02 ± 27.65	$-25,101.40 \pm 224.92$	-2.5477 ± 4.4885
3*	22.52 ± 154.01	$6,720.39 \pm 69.61$	159.61 ± 32.70	0.0507 ± 3.3785
4*	142.66 ± 7.86	$-4,970.87 \pm 88.25$	314.91 ± 42.28	0.9336 ± 4.2342
5*	123.74 ± 16.22	-185.03 ± 78.31	$-3,067.29 \pm 140.27$	3.5256 ± 2.2011
6*	-32.83 ± 116.85	$-30,211.61 \pm 114.46$	105.03 ± 58.16	4.1825 ± 3.8170
1	138.73 ± 4.56	$-31,341.37 \pm 95.91$	171.05 ± 53.47	3.9598 ± 2.8379
2	139.13 ± 4.29	232.69 ± 30.20	$-25,058.56 \pm 218.04$	2.0071 ± 2.3245
3	138.96 ± 4.40	$6,727.14 \pm 68.03$	158.19 ± 32.67	2.9723 ± 2.6404
4	138.91 ± 4.11	$-4,964.35 \pm 91.84$	315.53 ± 42.72	3.1643 ± 1.9206
5	139.49 ± 4.40	-177.91 ± 76.25	$-3,105.09 \pm 133.58$	2.6016 ± 2.3889
6	139.62 ± 4.48	$-30,186.22 \pm 112.32$	104.63 ± 59.91	1.1856 ± 2.8769
10 1-day arcs, clone50, estimation of calibration parameters only				
1	138.55 ± 4.77	$-31,335.71 \pm 370.74$	154.05 ± 73.17	3.8134 ± 2.4299
2	138.95 ± 4.51	231.95 ± 32.06	$-25,067.31 \pm 311.30$	1.8602 ± 1.9222
3	138.78 ± 4.61	$6,724.98 \pm 98.69$	141.34 ± 68.39	2.8263 ± 2.3171
4	138.72 ± 4.33	$-4,963.92 \pm 105.69$	298.51 ± 63.60	3.0188 ± 1.5024
5	139.31 ± 4.60	-178.64 ± 78.41	$-3,120.93 \pm 156.51$	2.4553 ± 2.0293
6	139.44 ± 4.68	$-30,180.60 \pm 358.92$	87.89 ± 89.00	1.0375 ± 2.5072
10 1-day arcs, clone50, co-estimation of 50×50 SH coefficients				
1	137.64 ± 4.09	$-31,322.48 \pm 685.88$	113.26 ± 27.59	3.5816 ± 2.5403
2	138.31 ± 3.82	224.60 ± 30.74	$-25,120.45 \pm 1713.61$	1.8725 ± 2.0062
3	137.98 ± 3.98	$6,725.05 \pm 127.33$	97.58 ± 40.43	2.6927 ± 2.4917
4	138.00 ± 3.65	$-4,963.19 \pm 125.42$	256.71 ± 23.34	2.8163 ± 1.6745
5	138.44 ± 3.92	-182.49 ± 74.26	$-3,145.82 \pm 197.04$	2.1873 ± 2.1989
6	138.78 ± 4.01	$-30,273.11 \pm 587.53$	38.88 ± 79.49	1.0445 ± 2.6261
10 1-day arcs, clone200, estimation of calibration parameters only				
1	139.97 ± 4.83	$-31,129.22 \pm 432.42$	161.67 ± 66.79	3.7768 ± 2.9809
2	140.37 ± 4.57	265.18 ± 62.24	$-25,030.40 \pm 1,958.83$	1.8376 ± 2.5903
3	140.19 ± 4.67	$6,723.19 \pm 121.54$	146.36 ± 56.37	2.7985 ± 2.8115
4	140.15 ± 4.47	$-4,902.36 \pm 122.46$	305.12 ± 68.24	2.9770 ± 2.2970
5	140.73 ± 4.75	-142.61 ± 89.09	$-3,104.35 \pm 189.87$	2.4230 ± 2.5917
6	140.85 ± 4.68	$-29,982.54 \pm 495.51$	91.28 ± 77.68	1.0203 ± 3.0552
10 1-day arcs, clone200, co-estimation of 80×80 SH coefficients				
1	137.38 ± 4.80	$-31,487.96 \pm 2,959.11$	85.27 ± 124.82	4.0291 ± 4.5808
2	137.98 ± 4.67	217.57 ± 62.67	$-27,676.22 \pm 9,802.25$	2.4668 ± 4.4927
3	137.69 ± 4.70	$6,764.73 \pm 563.35$	69.60 ± 120.18	3.2197 ± 4.5245
4	137.71 ± 4.37	$-5,004.83 \pm 532.81$	243.79 ± 60.45	3.3042 ± 3.9888
5	138.17 ± 4.53	-191.35 ± 129.41	$-3,518.45 \pm 1,427.72$	2.5841 ± 4.0761
6	138.47 ± 4.78	$-30,499.40 \pm 2,933.76$	6.57 ± 155.68	1.5780 ± 4.7898
20 1-day arcs, clone200, co-estimation of 80×80 SH coefficients				
1	134.19 ± 11.79	$-31,935.25 \pm 3,223.61$	66.92 ± 173.22	5.2292 ± 5.3334
2	134.69 ± 11.94	157.23 ± 125.62	$-26,816.06 \pm 12,840.06$	3.9328 ± 5.1451
3	134.21 ± 12.08	$6,875.51 \pm 597.89$	73.08 ± 152.69	5.0115 ± 5.4234
4	134.74 ± 11.46	$-5,149.76 \pm 624.99$	226.23 ± 99.82	4.1273 ± 5.3627
5	134.66 ± 12.09	-169.43 ± 164.86	$-3,500.17 \pm 1787.35$	4.4128 ± 5.3185
6	135.02 ± 12.03	$-30,962.06 \pm 3,112.04$	31.57 ± 192.61	3.2972 ± 5.2803

* Scale factor for X axis estimated

Table 7 Formal errors of accelerometer calibration parameters for 11 April 2008 based on a precision level of 10 cm for the time series of satellite x, y, z positions (nm/s^2 for biases and nm/s^2 per day for drifts, Δt denotes the estimation interval for the empirical accelerations)

Accelerometer 1 Δt	Bias X	Bias Y	Bias Z	Drift X	SF X	SF Y	SF Z
Scale factor for X axis estimated							
No emp.	1.74	15.55	3.55	0.2490	0.0430	0.0005	0.0013
1.5 h	8.98	272.73	6.32	1.3207	0.2284	0.0085	0.0172
1.0 h	22.39	490.27	10.49	3.4525	0.5683	0.0153	0.0335
0.5 h	32.51	953.76	23.98	5.1432	0.8229	0.0297	0.0715
Scale factor for X axis not estimated							
No emp.	0.05	15.25	3.55	0.0180	–	0.0005	0.0010
1.5 h	0.09	124.96	4.93	0.0265	–	0.0039	0.0072
1.0 h	0.18	476.50	9.47	0.2764	–	0.0149	0.0290
0.5 h	0.64	952.01	23.62	0.8241	–	0.0297	0.0699
80×80 gravity field co-estimated							
No emp. 10 days	1.85	3, 243.04	112.92	3.7311	–	0.1012	0.3176
No emp. 20 days	1.38	1, 554.48	59.43	2.5200	–	0.0486	0.1619
No empirical accelerations							
1	1.74	15.55	3.55	0.2490	0.0430	0.0005	0.0013
2	3.25	1.06	26.69	0.3249	0.0213	0.0005	0.0010
3	10.67	3.15	3.55	0.8592	0.0330	0.0005	0.0012
4	1.96	3.08	3.53	0.2493	0.0425	0.0005	0.0012
5	1.51	0.96	5.85	0.0328	0.0233	0.0005	0.0013
6	13.97	15.01	3.54	0.2324	0.0344	0.0005	0.0011
1	0.05	15.25	3.55	0.0180	–	0.0005	0.0010
2	0.05	0.75	26.67	0.0180	–	0.0005	0.0010
3	0.05	3.11	3.54	0.0180	–	0.0005	0.0010
4	0.05	2.70	3.52	0.0180	–	0.0005	0.0010
5	0.05	0.78	5.48	0.0180	–	0.0005	0.0011
6	0.05	14.84	3.54	0.0180	–	0.0005	0.0010

were also estimated in the presence of gravity field model errors: two so-called clones of the 200×200 EGM96 model were produced by adding spherical harmonic (SH) coefficient errors according to the estimated accuracy of the 200×200 combined GRACE model GGM02C (Tapley et al. 2005). The SH coefficient errors were obtained by multiplying the advertised coefficient errors with a value from a Gaussian random generator with expectation 0 and variance 1 (correlations were not taken into account, since the full covariance is not publicly available). In the first clone (referred to as "clone50"), only the SH coefficient errors to degree and order 50 were affected, whereas in the second clone ("clone200") this was the case to degree and order 200. For all cases, it was found that it was difficult to obtain convergence for estimating accelerometer scale factors for the X direction. Estimating those scale factors do more harm than good in the presence of the simulated gravity field model errors. It was argued before (e.g. Sect. 4.1.1) that it may be expected that especially the estimation of calibration parameters for the X axes would suffer from modeling errors. Therefore, no scale factors were estimated for the X axes in the presence of gravity field model

errors. Please note however that accelerometer biases (X, Y and Z axes) and drifts (X axis only) were estimated.

The RMS-about-mean for the daily scale factors is of the order of 0.011/0.010 and 0.014/0.076 for the Y/Z directions in the presence of SH errors to degree and order 50 and 200, respectively (Table 5, middle and bottom). It can be observed that with increasing gravity field model error, also the mean for especially the Y direction deviates more from 1: about 0.014 for SH coefficient errors up to degree and order 200, compared to less than 0.01 for coefficient errors up to degree and order 50. Obviously, gravity field model errors cause systematic deviations of the scale factors. The effect on the orbit accuracy is reflected by the increased RMS of fit of about 7 and 16 cm, respectively.

In principle, it is possible to estimate orbit, accelerometer calibration parameters and SH gravity field coefficients simultaneously. Ideally, the SH coefficients would absorb the gravity field model errors. First, for each individual accelerometer, a 50×50 SH expansion was co-estimated in the presence of only the 50×50 coefficient errors. It was found that this co-estimation already resulted in SH coefficient errors

Table 8 Estimated daily scale factors and their RMS-about-mean for the individual accelerometers

Acc.	SF Y	SF Z	Orbit (cm)
Δt = 1.5 h			
1	1.003 ± 0.104	0.996 ± 0.760	5.40
2	1.007 ± 0.107	0.966 ± 0.763	5.32
3	1.008 ± 0.106	0.992 ± 0.772	5.38
4	1.008 ± 0.109	0.994 ± 0.743	5.31
5	1.008 ± 0.106	0.979 ± 0.753	5.29
6	1.010 ± 0.108	0.963 ± 0.773	5.32
Δt = 1.0 h			
1	0.980 ± 0.034	1.034 ± 0.071	1.17
2	0.102 ± 0.034	1.008 ± 0.065	1.14
3	1.001 ± 0.032	1.026 ± 0.070	1.14
4	0.996 ± 0.041	1.030 ± 0.068	1.15
5	1.000 ± 0.036	1.031 ± 0.070	1.15
6	1.023 ± 0.031	1.019 ± 0.069	1.14
Δt = 0.5 h			
1	0.989 ± 0.014	1.010 ± 0.014	0.32
2	1.001 ± 0.014	0.979 ± 0.015	0.32
3	0.997 ± 0.014	1.007 ± 0.015	0.32
4	0.997 ± 0.014	1.009 ± 0.015	0.32
5	0.998 ± 0.014	1.010 ± 0.014	0.32
6	0.995 ± 0.014	1.005 ± 0.015	0.32

The full 200×200 gravity field model error is taken into account, and radial and cross-track 1-cpr empirical accelerations are co-estimated with the orbital and accelerometer calibration parameters

larger than the original errors based on the GGM02C model (Fig. 2). This is due to the accelerometer observation errors that affect not only the accelerometer calibration parameters, but also the SH coefficients and due to the fact that only a 10-day period was used. It has to be noted that it is anticipated that GOCE will perform very well at short spatial wavelengths, but relatively poor at long wavelengths. In fact, it is anticipated that GOCE will not lead to significant improvements for SH coefficients below degree 50 compared to GRACE (Visser 1999). In addition, the RMS-about-mean of the daily scale factors deteriorates significantly up to 0.073 for the Z direction (Table 5). Finally, when using the estimated SH coefficients in new orbit determinations, the orbit fit improved from about 7 cm to 0.8–1.5 cm. Thus despite the SH coefficient errors, accurate orbits can be computed, which is due to the fact that these coefficient errors are compensated by errors in the estimated accelerometer calibration parameters. When including SH coefficient errors up to degree and order 200 and estimating SH coefficients to degree and order 80, the RMS-about-mean deteriorates even much more up to 0.09/0.42 for the Y/Z directions. Especially for a high-precision full 80×80 gravity field recovery, a

10-day period is rather short. However, it can be seen that the RMS-about-mean does not improve when using a 20-day period, which can be explained by the fact that the gravity field errors for the SH coefficients above degree 80 cause systematic orbit errors that alias into the estimated accelerometer calibration parameters and SH coefficients. It can be argued that for a shorter period (i.e. 10 days) such omission errors can be absorbed better by the estimated parameters (SH coefficients, orbit and calibration parameters) than for a longer period (i.e. 20 days). This is also reflected by the orbit fit when the estimated SH coefficients are used: for the 10-day period the improvement is from 16 cm to about 3 cm, whereas for the 20-day period the orbit fit is about 9 cm (Table 5). Even without omission errors, e.g. for the case where SH coefficients were corrupted up to degree and order 50, the RMS-about-mean for the calibration parameters does not improve when estimating SH coefficients to degree and order 50 as well. It can thus be concluded that a co-estimation of accelerometer calibration parameters and SH gravity field coefficients does not lead to a better estimation of the accelerometer calibration parameters themselves with the current parameterization. This is also reflected by a significant increase of the formal errors of the accelerometer calibration parameters (Table 7). It might be argued as well that the GRACE mission has already resulted in a very precise long to medium wavelength gravity field model and further improvements are anticipated as more and more observations are accumulated. In addition, the GOCE mission itself will provide satellite gravity gradient observations that contain high-quality medium to short wavelength gravity field information. It is anticipated that an integrated approach can be adopted where both GOCE orbit solutions and gravity gradients are used simultaneously to estimate calibration parameters and SH coefficients (Visser 2007a).

In practice, typically a number of empirical accelerations at the orbital resonance frequencies are included in the set of estimated parameters as well (Table 1). These parameters are very efficient in absorbing dynamic force model errors, whether caused by gravity field model errors or other force model errors. This is a procedure used often when estimating accelerometer calibration parameters whether in combination with gravity field coefficients or not (Tapley et al. 2005; van den IJssel and Visser 2003). Therefore, a number of additional estimations were done as well, using different time intervals for estimated empirical accelerations (Table 8). The selected empirical accelerations are radial and cross-track 1-cpr accelerations (4 per set). It was found that accelerometer scale factors could be obtained with mean values that deviate in general less than 0.01 from 1 with an RMS-about-mean of around 0.015 when the time interval of the empirical accelerations is 30 min (Table 8). Thus, more accurate and more stable scale factor values are obtained when estimating empirical accelerations instead of gravity SH coefficients.

Table 9 Estimated biases (nm/s^2) and drifts (nm/s^2 per day) for the individual accelerometers

Acc.	Bias X	Bias Y	Bias Z	Drift X
$\Delta t = 1.5$ h				
1	137.72 ± 3.88	$-31,702.37 \pm 3,339.65$	96.91 ± 168.90	3.2467 ± 3.0876
2	138.27 ± 3.74	218.15 ± 59.14	$-24,397.16 \pm 19,610.89$	1.1688 ± 2.6041
3	137.99 ± 3.81	$6,826.43 \pm 674.86$	90.43 ± 214.29	2.2825 ± 2.9398
4	138.02 ± 3.48	$-5,068.30 \pm 606.01$	240.17 ± 64.68	2.4523 ± 2.1911
5	138.46 ± 3.67	-198.89 ± 105.56	$-3,071.76 \pm 2,557.24$	1.9340 ± 2.5823
6	138.73 ± 3.88	$-30,758.56 \pm 3,383.97$	43.92 ± 283.60	0.4321 ± 3.0394
$\Delta t = 1.0$ h				
1	137.70 ± 4.01	$-30,968.56 \pm 1,103.97$	96.61 ± 39.82	3.1516 ± 2.8994
2	138.14 ± 3.83	211.68 ± 34.63	$-25,471.32 \pm 1,663.40$	1.4608 ± 2.5037
3	137.91 ± 3.91	$6,780.60 \pm 201.41$	87.34 ± 35.97	2.3308 ± 2.7476
4	137.95 ± 3.66	$-5,004.31 \pm 227.82$	245.57 ± 26.22	2.4981 ± 2.2956
5	138.42 ± 3.88	-195.47 ± 86.89	$-3,237.89 \pm 276.74$	1.9345 ± 2.5539
6	138.63 ± 4.00	$-31,177.40 \pm 982.45$	31.83 ± 67.49	0.6469 ± 2.9027
$\Delta t = 0.5$ h				
1	137.68 ± 4.24	$-31,240.48 \pm 470.95$	105.47 ± 35.14	3.2330 ± 2.6777
2	138.46 ± 4.04	220.44 ± 27.59	$-24,730.24 \pm 359.34$	1.4446 ± 2.2210
3	138.04 ± 4.14	$6,757.15 \pm 102.89$	95.38 ± 28.23	2.3861 ± 2.4900
4	137.97 ± 3.84	$-5,008.26 \pm 116.40$	250.76 ± 25.87	2.5623 ± 1.8549
5	138.26 ± 4.12	-192.97 ± 80.49	$-3,160.44 \pm 143.06$	2.0147 ± 2.3454
6	138.87 ± 4.21	$-30,309.29 \pm 434.96$	39.46 ± 61.53	0.6548 ± 2.6733

The full 200×200 gravity field model error is taken into account ("clone200"), and radial and cross-track 1-cpr empirical accelerations are co-estimated with the orbital and accelerometer calibration parameters (Δt denotes the estimation interval for the empirical accelerations)
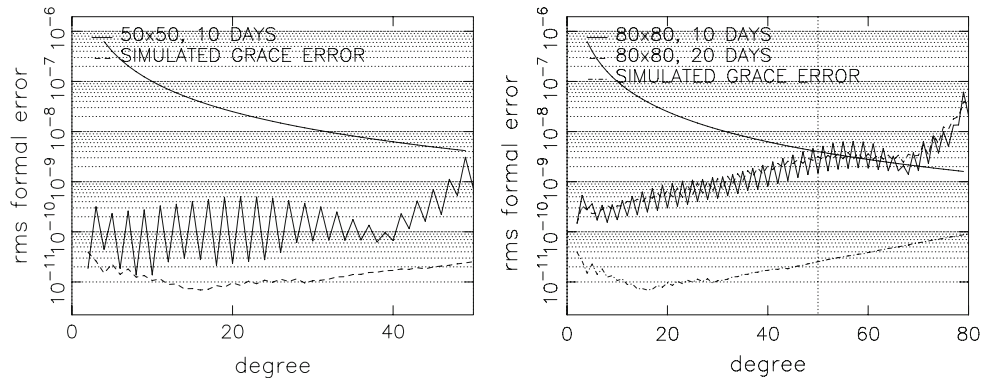

Fig. 2 Gravity field recovery errors from combined estimation with daily orbit and calibration parameters in the presence of either 50×50 or 200×200 SH model error. The displayed errors hold for accelerometer 1 (similar gravity field recovery errors were obtained for the other accelerometers). The decaying line denotes the gravity field signal according to Kaula's rule of thumb (Kaula 1966)

Also, lower RMS-about-mean values for the accelerometer bias estimates are obtained when estimating this many empirical accelerations (Table 9). The higher stability is also consistent with the significantly lower formal errors when estimating empirical accelerations instead of SH coefficients (Table 7).

5 Conclusions

A method has been implemented and tested for estimating calibration parameters for the six individual GOCE accelerometers by precise orbit determination. For each accelerometer, a separate orbit determination is carried out during which biases, drifts and scale factors can be estimated for all three axes. This is opposed to the baseline method for GOCE gravity field determination, where CM accelerometer observations from the sensitive axes will be used. However, the primary objective was to assess the possibility of estimating calibration parameters for all six individual accelerometers. This cannot be achieved by taking CM accelerometer observations only, even if also the less sensitive axes are used. It was found though that similar results were obtained for all CM combinations. Based on

the results obtained with CM accelerometer observations, it was concluded that it was helpful to estimate accelerometer drifts for the X axes. Moreover, COM corrections led to scale factors that were much closer to 1 for the X axis.

When using individual accelerometer observations, it was found that the accelerometer observations needed to be corrected for rotational terms and gravity gradients due to the center-of-mass offsets of these accelerometers. Rotational corrections were successfully derived from the noisy star tracker observations and a low-degree gravity field model was found to be sufficient for deriving the gravity gradient corrections. When using an error-free gravity field model in the precise orbit determination, scale factor values were obtained very close to 1 for the Y and Z axes, where all other anticipated error sources, such as colored accelerometer observation noise, biases and accelerometer drifts, were modeled in great detail in the End-to-End simulation. The deviations from 1 are in general smaller than 0.01. For the X axes, the estimated scale factors deviated significantly from 1 and in fact no reliable estimates could be obtained. This can be explained by the DFC, which leaves a very small signal for the X axes. This results in formal errors that are an order of magnitude larger than for the Y and Z axes, again an indication that an accurate determination of the scale factors for the X axes is difficult and very sensitive to observation noise and for example force model errors.

When introducing gravity field model errors, which are of the order of the claimed accuracy of GRACE models, this results in significantly less accurate accelerometer calibration parameters, although still scale factors can be obtained with an accuracy of the order of 0.01 when averaged over a 10-day period. It was found that simultaneous estimation of accelerometer calibration parameters and gravity field coefficients from merely GOCE orbit solutions does not result in improved accelerometer scale factor values when using a data period of 10, and also 20 days. Improvements might be anticipated when gravity gradient observations are used as well. However, accurate and stable accelerometer scale factors could be obtained when co-estimating a sufficient number of empirical accelerations, an approach typically used in the processing of real accelerometer observations.

References

Alenia (1999) GOCE: Gravity field and ocean circulation explorer. Phase A, Summary Report, ESA Contract 13028/98/NL/GD, Alenia Aerospazio

Banfi E, Marradi L, Moretto M (2000) The LAGRANGE TM GNSS receiver for scientific applications. In: Schürmann B (ed) Data systems in aerospace, vol 457. ESA Special Publication, pp 279–286

Bock H, Jaeggi A, Svehla D, Beutler G, Hugentobler U, Visser P (2007) Precise orbit determination for the GOCE satellite using GPS. Adv. Space Res. 39(10):1638–1647, doi:10.1016/j.asr.2007.02.053

Bouman J, Koop R, Tscherning C, Visser P (2004) Calibration of GOCE SGG data using high-low SST, terrestrial gravity data, and global gravity field models. J Geod 78(1–2): 124–137

Bruinsma S, Biancale R (2003) Total densities derived from accelerometer data. J Spacecr Rockets 40(2): 230–236

Bruinsma S, Tamagnan D, Biancale R (2004) Atmospheric densities derived from CHAMP/STAR accelerometer observations. Planet Space Sci 52(4):297–312, doi:10.1016/j.pss.2003.11.004

Catastini G, Cesare S, De Sanctis S, Dumontel M, Parisch M, Sechi G (2006) Predictions of the GOCE in-flight performances with the end-to-end system simulator. In: 3rd GOCE User Workshop, 6–8 November 2006, Frascati, Italy, pp 9–16, ESA SP-627

Cesare S (2005) Performance requirements and budgets for the gradiometric mission. Technical Note, GOC-TN-AI-0027, Issue 3, Alenia Spazio, Turin, May 2005

Cesare C, Catastini G (2005) Gradiometer on-orbit calibration procedure analysis. Technical Note to ESA, GO-TN-AI-0069, Issue 3, Alenia Aerospazio

Clohessy WH, Wiltshire RS (1960) Terminal Guidance System for Satellite Rendezvous. J Aerospace Sci 27(9):653–658, 674

Drinkwater M, Haagmans R, Muzzi D, Popescu A, Floberghagen R, Kern M, Fehringer M (2007) The GOCE gravity mission: ESA's first core explorer. In: 3rd GOCE User Workshop, 6–8 November 2006, Frascati, Italy, pp 1–7, ESA SP-627

ESA (1999) Gravity field and steady-state ocean circulation mission. Reports for Mission Selection, The Four Candidate Earth Explorer Core Missions, SP-1233(1), European Space Agency

GSFC (2002) GRACE: the gravity recovery and climate experiment. NASA Facts, National Aeronautics and Space Administration, Goddard Space Flight Center FS-2002-1-029-GSFC

van den IJssel J, Visser PNAM (2003) CHAMP precise orbit determination using GPS data. Adv Space Res 31(8): 1889–1895

Kaula WM (1966) Theory of satellite geodesy. Blaisdell Publishing Co., Waltham

Koop R, Gruber T, Rummel R (2006) The status of the GOCE high-level processing facility. In: 3rd GOCE User Workshop, 6–8 November 2006, Frascati, Italy, pp 199–205, ESA SP-627

Lemoine FG, Kenyon SC, Factor JK, Trimmer RG, Pavlis NK, Chin DS, Cox CM, Klosko SM, Lutchke SB, Torrence MH, Wang YM, Williamson RG, Pavlis EC, Rapp RH, Olsen TR (1998) The development of the joint NASA GSFC and the national imagery and mapping agency (NIMA) Geopotential Model EGM96. NASA/TP-1998-206861

Montenbruck O, Gill E (2000) Satellite orbits—models methods applications. Springer, Heidelberg, ISBN 3-540-67280-X

Pavlis DE, Poulouse S, McCarthy JJ (2006) GEODYN operations manual. Contractor report, SGT Inc., Greenbelt

Reigber Ch, Schwintzer P, Lühr H (1999) The CHAMP geopotential mission. In: Marson I, Sünkel H (eds) Bollettino di Geofisica Teoretica ed Applicata, vol 40, No. 3–4. Proceedings of the 2nd joint meeting of the international gravity and the international geoid commission, Trieste 7–12 September 1998, ISSN 0006-6729, pp 285–289

Reigber C, Schwintzer P, Neumauer K-H, Barthelmes F, König R, Förste Ch, Balmino G, Biancale R, Lemoine J-M, Loyer S, Bruinsma S, Perosanz F, Fayard T (2003) Earth gravity field model EIGEN-2. Adv Space Res 31(8): 1883–1888

Tapley B, Ries J, Bettadpur S, Chambers D, Cheng M, Condi F, Gunter B, Kang Z, Nagel P, Pastor R, Pekker T, Poole S, Wang F (2005) GGM02: an improved earth gravity field model from GRACE. J Geod 79(8):467–478, doi:10.1007/s00190-005-0480-z

Visser PNAM (1999) Gravity field determination with GOCE and GRACE. Adv Space Res 23(4): 771–776

Visser PNAM, IJssel Jvan den , Koop R, Klees R (2001) Exploring gravity field determination from orbit perturbations of the european gravity mission GOCE. J Geod 75(2/3): 89–98

Visser PNAM, van den IJssel J (2003) Verification of CHAMP accelerometer observations. Adv Space Res 31(8): 1905–1910

Visser PNAM, IJssel J van den, Van Helleputte T, Bock H, Jaeggi A, Beutler G, Hugentobler U, Svehla D (2006) Rapid and precise orbit determination for the GOCE satellite. In: 3rd GOCE User Workshop, 6–8 November 2006, Frascati, Italy, pp 235–239, ESA SP-627

Visser PNAM (2007a) GOCE gradiometer validation by GPS. Adv Space Res 39(10):1630–1637, doi:10.1016/j.asr.2006.09.014

Visser PNAM (2007 b) Exploring the possibilities for star-tracker-assisted validation of the six individual GOCE accelerometers. J Geod Online First (doi:10.1007/s00190-007-0205-6), pp 1–10